

**Exploring High Molecular Weight Vinyl Ester Polymers made
by PET-RAFT**

Journal:	<i>Polymer Chemistry</i>
Manuscript ID	PY-ART-01-2024-000065
Article Type:	Paper
Date Submitted by the Author:	18-Jan-2024
Complete List of Authors:	Weerasinghe, M.; Miami University, Chemistry and Biochemistry De Alwis Watuthanthrige, Nethmi; Miami University, Department of Chemistry and Biochemistry; ETH Zurich, department of Materials Konkolewicz, Dominik; Miami University, Chemistry and Biochemistry

Exploring High Molecular Weight Vinyl Ester Polymers made by PET-RAFT

M. A. Sachini N. Weerasinghe, Nethmi De Alwis Watuthanthrige, Dominik Konkolewicz*

Department of Chemistry and Biochemistry, Miami University, 651 E High St, Oxford, OH, 45056

* Corresponding Author: d.konkolewicz@miamiOH.edu

Abstract

Polyvinyl esters have wide range of applications; however, the synthesis of high molecular weight uniform polymers is an ongoing challenge. Vinyl ester monomers are among the less activated monomers compatible with RAFT polymerization. The highly reactive unconjugated radicals formed during propagation are prone to side reactions, especially irreversible transfer, limiting the evolution of molecular weight and control over molecular weight distribution. Herein, the effect of monomer type on the control of polyvinyl esters synthesized by photoinduced electron/energy transfer reversible addition-fragmentation chain transfer polymerization (PET-RAFT) is explored. We show that PET-RAFT is capable of forming high molecular weight polyvinyl esters (Vinyl Pivalate: $M_n > 350,000$ and Vinyl Acetate: $M_n > 80,000$) under mild conditions. The livingness of the polymerization was determined by following chain extensions for low DP and high DP systems.

Introduction

The function and properties of polymeric materials are highly dependent on the molecular weight, and certain applications require control over the chain length and distribution.¹⁻³ Polyvinyl esters have numerous applications, both fundamental and industrial. For instance, poly(vinyl acetate) is used as an adhesive for various substrates, and as powder additives for construction materials.⁴ Polyvinyl esters are also precursors for poly(vinyl alcohol) which is important as a coating material.⁵ Vinyl esters can be polymerized using

conventional free radical polymerization (FRP). Due to the limited stabilization of their propagating radicals, vinyl esters are considered as less activated monomers.^{6,7} The poor stabilization of the propagating radicals of vinyl esters results in a high level of irreversible chain transfer reactions to monomers, to propagating chains (intermolecular and intramolecular) and to solvent when compared with other monomers.⁸⁻¹⁰ Furthermore, during the polymerizations vinyl ester monomers can add in head-to-head manner to the propagating chain, creating irregularities in the polymer backbone.¹¹

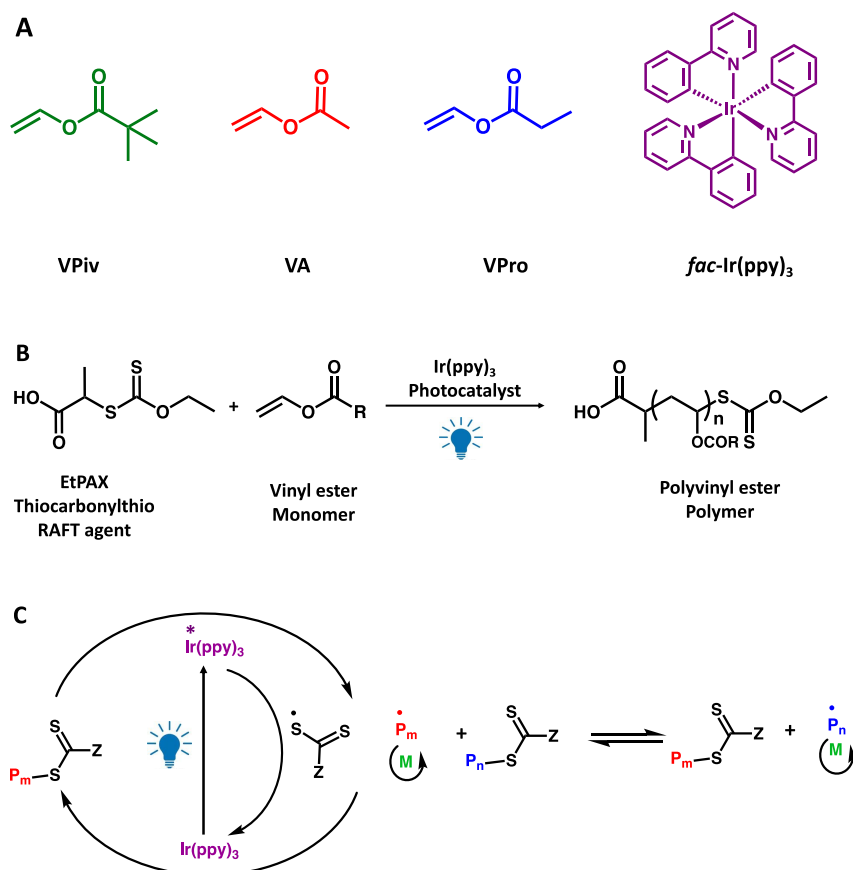
Reversible deactivation radical polymerization methods (RDRP) have been developed over the past 2-3 decades to improve the control over polymer structure, while maintaining similar tolerance to monomer functionality as FRP. Various RDRP methods such as iodine transfer polymerization (ITP)^{12,13}, atom transfer radical polymerization (ATRP)^{14,15}, organometallic-mediated radical polymerization¹⁶ and reversible addition fragmentation chain transfer polymerization (RAFT) have been developed to control the molecular weights and molecular weight distributions (MWDs) of polymers.¹⁷⁻¹⁹ Matyjaszewski and coworkers have obtained first well controlled vinyl acetate polymers using the living radical polymerization in the presence of ternary complexes of organoaluminium compounds with Lewis bases and stable radicals. However, the number average molecular weight (M_n) was limited to $\sim 30,000$ although relatively narrow dispersity were found ($M_w/M_n < 1.3$).²⁰ The vast majority of controlled vinyl ester polymerizations are based on the RAFT process. RAFT is one of the more versatile methods for imparting living characteristics to radical polymerization.^{21,22} RAFT polymerization of vinyl acetate has been performed as bulk or solution polymerization. Schork and coworkers have studied RAFT miniemulsion polymerization of vinyl acetate and the maximum value reported was 80,000 with high dispersity ($M_w/M_n \sim 2.60$).²³ Cunningham and coworkers have synthesized poly(vinyl acetate) homopolymers with M_n around 160,000 and relatively broad dispersity ($M_w/M_n \sim 2.0$) using xanthate mediated RAFT miniemulsion

polymerization.²⁴ Zhao and coworkers have studied the synthesis of high molecular weight of poly(vinyl acetate) in emulsion polymerization using a novel water soluble N,N-dialkyl dithiocarbamate RAFT agent. The maximum M_n obtained was $\sim 160,000$ with a high dispersity ($M_w/M_n \sim 2.50$).²⁵

Traditionally, RAFT polymerization involves thermally generated radicals, typically from azo based initiators.^{21,22} However, recently RAFT reactions that use photochemically generated radicals have been developed.²⁶ Sumerlin and coworkers have obtained ultra-high molecular weight acrylic type polymer by following photo mediated polymerization approach under UV and sunlight.²⁷ Photochemical processes are compatible with lower temperatures, potentially reducing the impact and rate of side reactions compared to thermal RAFT polymerization.²⁸ Britton and coworkers have found that high temperature conditions in emulsion free radical polymerization of vinyl acetate can increase the branching in the polymer.²⁹ Furthermore, it has been discussed that the relative abundance of head-to-head addition can be increased with temperature.¹¹ In particular, photoinduced electron/energy transfer RAFT (PET-RAFT) uses photocatalysts to generate radicals which then participate in propagation and reversible transfer through the RAFT process. In PET-RAFT, the photocatalyst is excited in the presence of light. The excited photocatalyst reacts with the RAFT chain transfer agent (CTA) either through an energy or electron transfer process, returning the photocatalyst to the ground state and cleaving the CTA to a propagating radical. In this PET-RAFT polymerization, the CTA acts as both, chain initiating species for radical generation and reversible transfer agent through the RAFT process. There are many advantages of PET-RAFT reaction over conventional RAFT.³⁰ PET-RAFT can be performed under mild reaction conditions, using visible light which can be a greener energy source. Additionally, spatiotemporal control can be introduced by changing when and where a light is irradiated.^{28,31–}

³³ Moreover, PET-RAFT polymerization is capable of polymerizing both conjugated

monomers (styrene and methyl acrylate) and unconjugated monomers (vinyl esters). Boyer and coworkers have studied PET-RAFT polymerization of vinyl acetate and N-vinyl pyrrolidinone and their oxygen tolerance studies. They have synthesized poly(vinyl acetate) polymer with $M_n \sim 100,000$ and poly(N-vinyl pyrrolidinone) with $M_n \sim 40,000$.²⁸ However, high molecular weights, greater than 100,000 were not explored in their study. Due to the critical importance of high molecular weight polymers, it is necessary to explore the full scope of molecular weights achievable by PET-RAFT. Here, we studied the polymerization of three different vinyl ester monomers: vinyl propionate (VPro); vinyl acetate (VA); and vinyl pivalate (VPiv) exploring their kinetics under PET-RAFT conditions and the molecular weights achievable in these systems. Especially, the evolution of molecular weights, and MWDs with changing the targeted chain length was studied for three different vinyl ester monomers. The monomers explored and the photocatalyst are given in Scheme 1A, with general polymerization reaction given in Scheme 1B, and the proposed PET-RAFT mechanism shown in Scheme 1C.



Scheme 1: (A) The monomers and the photocatalyst used. (B) General polymerization reaction. (C) The proposed PET-RAFT mechanism.

Results and Discussion

This work explores the effect of vinyl ester monomer structure on the control and molecular weights of polyvinyl esters synthesized by PET-RAFT polymerization using $\text{Ir}(\text{ppy})_3$ as a photocatalyst. As shown in Scheme 1B, EtPAX was selected as the CTA which is capable of polymerizing less activated monomers like vinyl esters. Because, EtPAX like xanthate RAFT agents are capable of controlling the polymerization of vinyl esters by increasing the electron density of the RAFT adduct, destabilizing the RAFT adduct and thereby making high reactive vinyl ester propagating group to leave the RAFT adduct to continue the polymerization.^{34–36} All reactions were carried out as bulk polymerizations at room temperature, under deoxygenated conditions and blue light (Intensity = $7.9 \pm 0.4 \text{ mW/cm}^2$, $\lambda_{\text{max}} = 450 \pm 10 \text{ nm}$)³⁷ irradiation using $\text{Ir}(\text{ppy})_3$ photocatalyst (Concentration of $\text{Ir}(\text{ppy})_3$ stock solution = 1000 ppm) as depicted in Scheme 1C. Initially, three different concentrations of photocatalyst (3, 10 and 30 ppm relative to monomer) were tested for the polymerization. As seen in Figure S1, 3 ppm resulted in very slow polymerization, reaching a conversion below 3% after 15 h of polymerization time. In contrast, both 10 ppm and 30 ppm systems showed similar polymerization kinetics. However, 10 ppm system was selected as the most suitable low photocatalyst concentration for the PET-RAFT polymerization of vinyl esters in this work because it has the ability to synthesize higher molecular weight polymers with narrow dispersity when compared to 30 ppm system as given in Table S2.

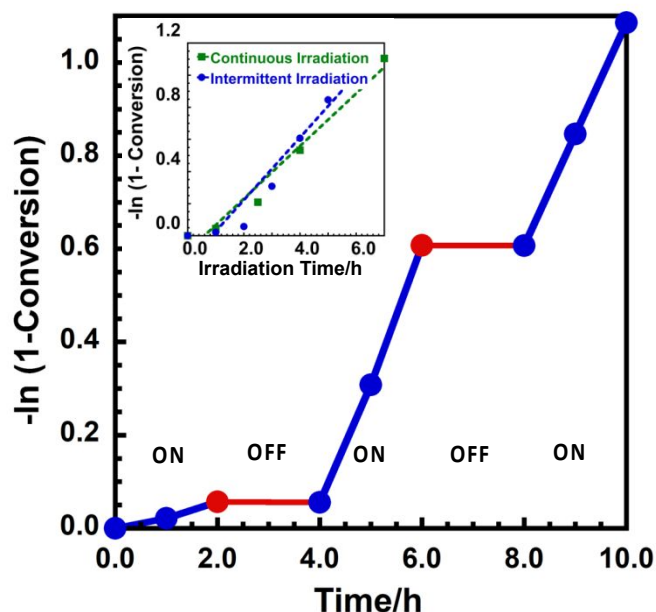


Figure 1: Semilogarithmic kinetics plot for light ON-OFF experiments of VPiv monomer for (Degree of Polymerization) DP 200 with continuous and intermittent blue light irradiation at room temperature, using a molar ratio of $[\text{VPiv}]:[\text{EtPAX}]:[\text{Ir}(\text{ppy})_3] = 200:1:0.002$.

To explore the effect of the blue light for the polymerization, an ON-OFF experiment was performed. As in Figure 1, the VPiv monomer undergoes efficient polymerization under blue light but ceases polymerization almost instantaneously when the light source is turned off.³³ Polymerization resumes efficiently once the blue light source is turned on again. Figure 1 inset compares the polymerization kinetics under continuous irradiation, to the polymerization kinetics in the intermittent irradiation (ON-OFF) experiment, where only the irradiated time is considered. The inset of Figure 1 shows that there is essentially no difference in the polymerization rates between continuous irradiation and intermittent irradiation. When considering both graphs in Figure 1, it indicates the photochemical control of the PET-RAFT process, and polymerization reaction can be controlled by changing light ON and OFF process, with the underlying radical generation process being photochemically controlled.

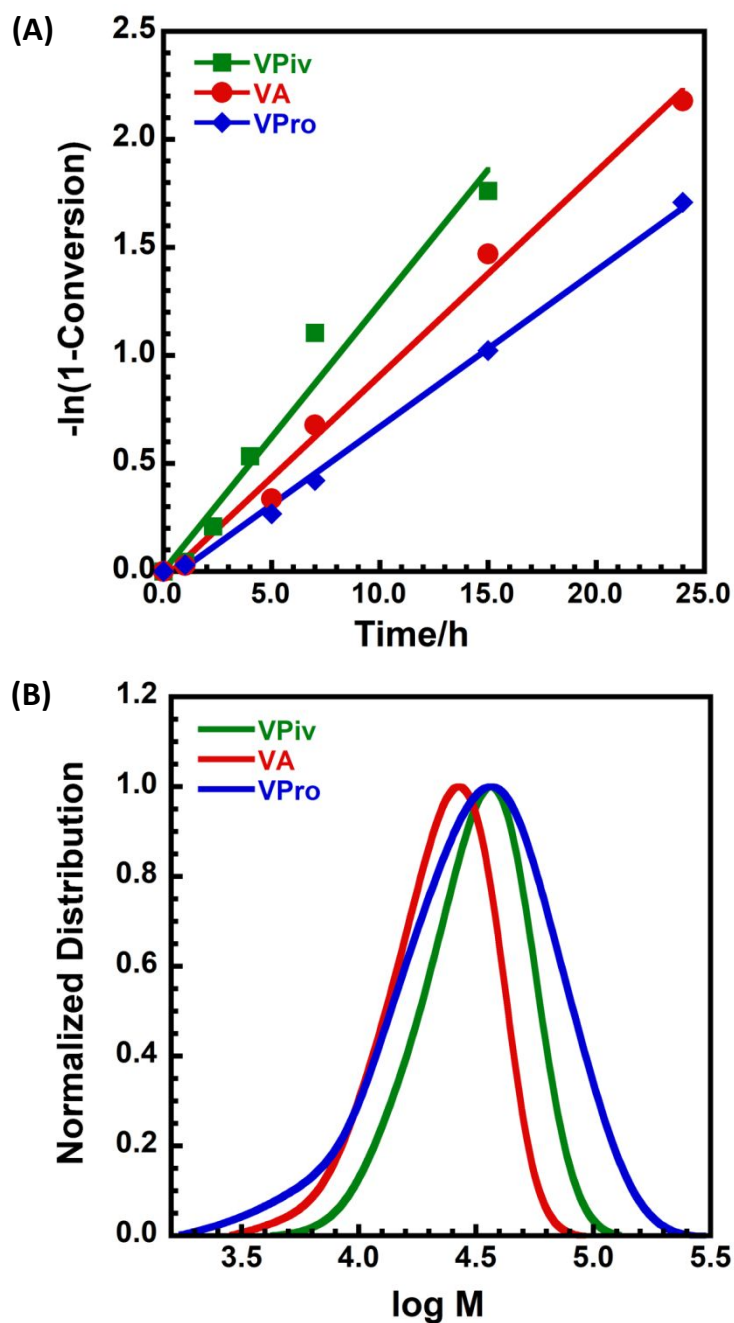
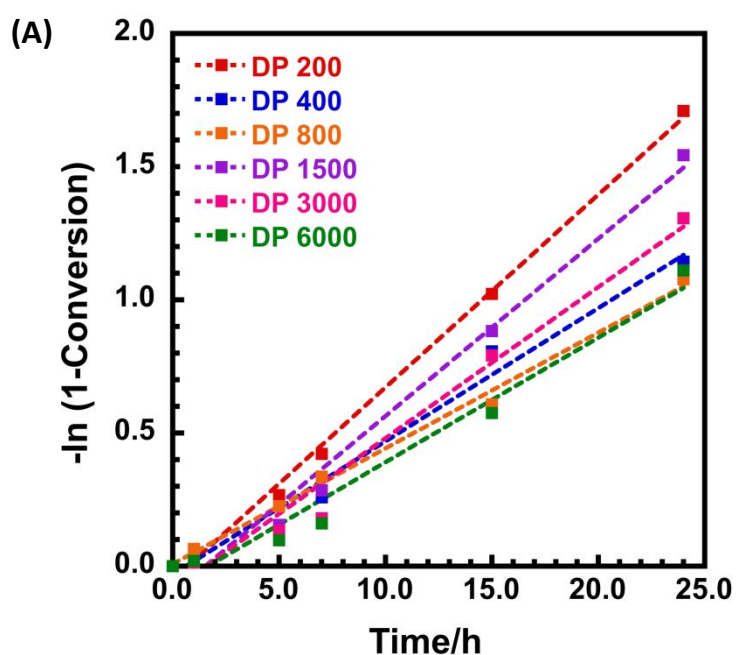


Figure 2: (A) Semilogarithmic kinetics plots for polymerization of VPiv, VA and VPro monomers for DP 200. (B) Molecular weight distributions for each monomer. Polymerization reactions were performed at room temperature and under blue light irradiation, using a molar ratio of $[\text{Monomer}]:[\text{EtPAX}]:[\text{Ir}(\text{ppy})_3] = 200:1:0.002$.

The polymerization rate for all three vinyl ester monomers were studied under established conditions, of monomer:EtPAX = 200:1, to determine the polymerization efficiency and control over the reaction. Figure 2A shows the kinetic data comparison for each

monomer. VPiv monomer showed the fastest polymerization with an apparent rate of propagation $k_p^{\text{app}} = 0.0021 \text{ min}^{-1}$, VA has the second highest $k_p^{\text{app}} = 0.0016 \text{ min}^{-1}$. The rate of polymerization decreases notably with VPro having $k_p^{\text{app}} = 0.0012 \text{ min}^{-1}$. As seen in Figure 2B, the MWDs of both PVPiv and PVA polymers were relatively narrow. PVPiv gave $M_w/M_n = 1.30$ and PVA gave $M_w/M_n = 1.34$ at the end points. However, PVPro had a broader dispersity, with $M_w/M_n = 1.86$. Therefore, the DP 200 systems of VPiv and VA monomers are well controlled, whereas the VPro system showed relatively poor control over the polymer.



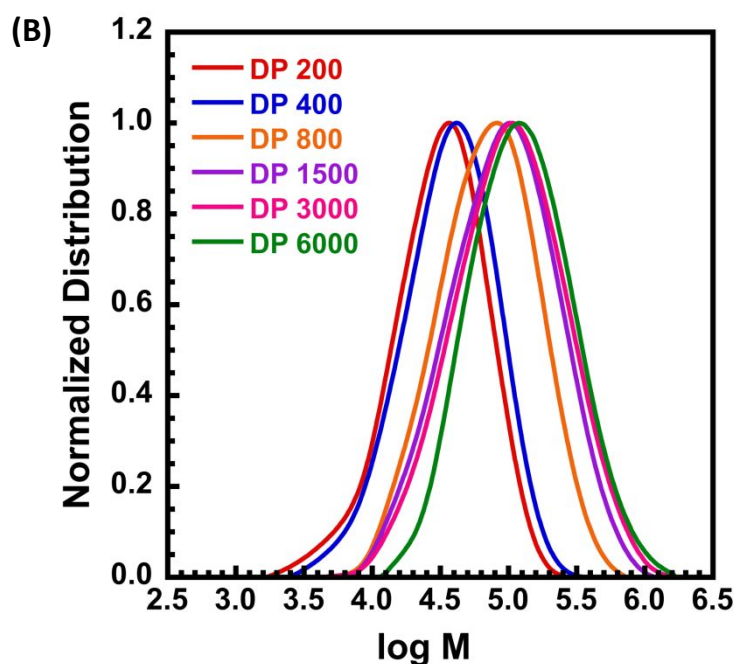


Figure 3: (A) Semilogarithmic kinetic plots for PVPro. (B) Molecular weight distributions of PVPro. Polymerization reactions were performed at room temperature and under blue light irradiation, using a molar ratio of $[\text{Ir}(\text{ppy})_3]/[\text{VPro}] = 10$ ppm and $[\text{VPro}]:[\text{EtPAX}] = X:1$ ($X =$ The value of DP, e.g., for DP 200, $X = 200$).

The polymerization of VPro was studied under blue light and at room temperature targeting ratios of VPro:EtPAX from 200:1 to 6000:1. Figure 3A shows the kinetic data for the polymerization of VPro. As seen in Figure 3A, the DP 200 system showed the highest polymerization rate. All other polymerization rates for higher DP values were lower than the DP 200 system. However, there was no systematic trend in the polymerization rate with increasing ratio of VPro:EtPAX. Figure 3B shows the MWDs of these polymers with different ratios of VPro:EtPAX. Although the M_n increased with higher VPro:EtPAX ratio, there was minimal increase in molecular weight above a ratio of VPro:EtPAX = 800:1. As shown in Table 1, the highest M_n value achieved for PVPro was $\sim 89,000$ and M_w/M_n was closer to 2 for each ratio of VPro:EtPAX. In addition to that PVPro polymers with $M_n = 49,300$ with $M_w/M_n = 1.43$ and $M_n = 64,300$ with $M_w/M_n = 1.62$ were obtained for DP 6000 at 7 h and 15 h reaction time respectively as relatively high molecular weight polymers with low dispersity as seen in

Table S7. These results overall indicate that VPro is a monomer that is unlikely to be useful for the synthesis of high molecular weight well-controlled polyvinyl esters.

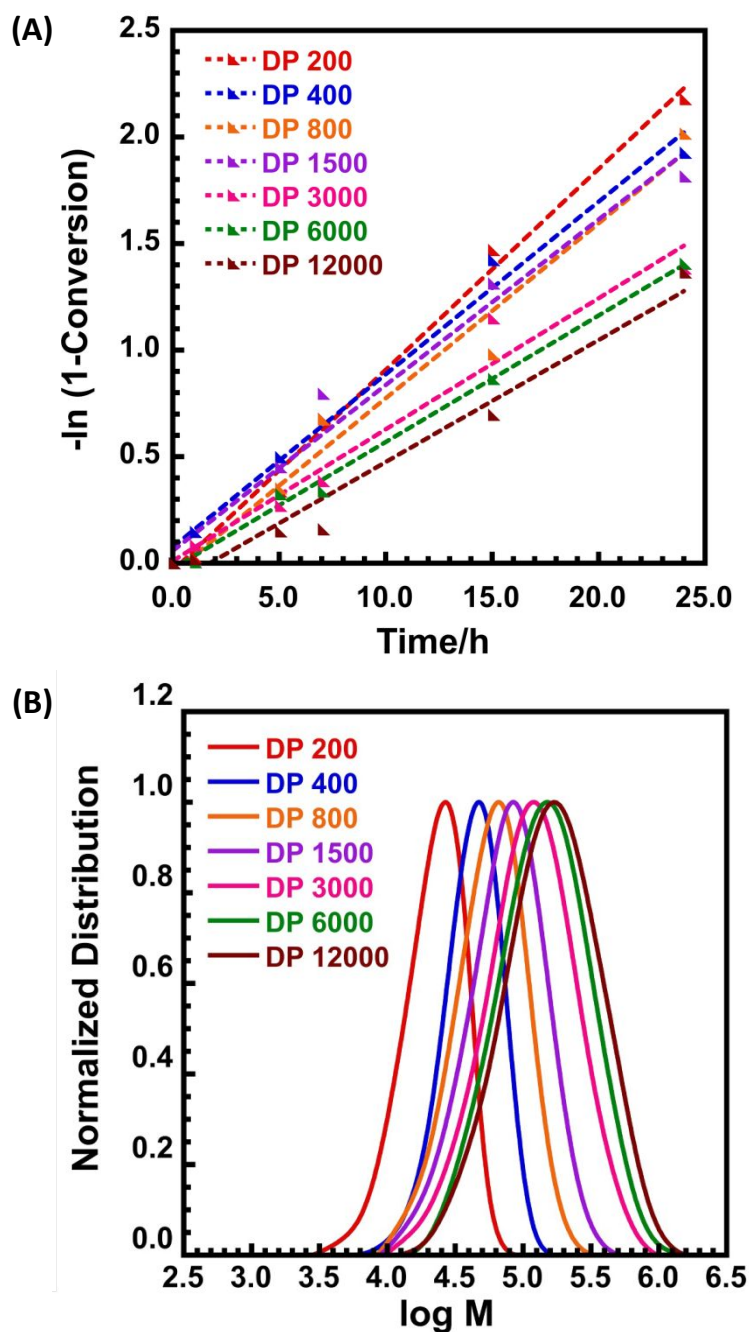
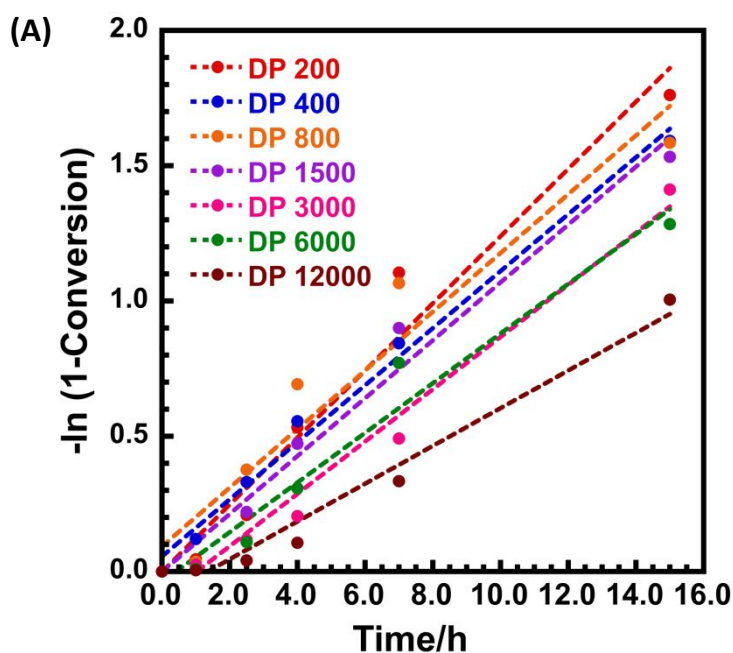


Figure 4: (A) Semilogarithmic kinetic plots for PVA. (B) Molecular weight distributions of PVA. Polymerization reactions were performed at room temperature and under blue light irradiation, using a molar ratio of $[\text{Ir}(\text{ppy})_3]/[\text{VA}] = 10$ ppm and $[\text{VA}]:[\text{EtPAX}] = X:1$ ($X =$ The value of DP, e.g., for DP 200, $X = 200$).

Figure 4A shows the kinetic data for the polymerization of VA with VA:EtPAX ratio ranging from 200:1 to 12000:1. As the target chain length increases, the reaction rate decreases due to the lower concentration of CTA for activation. Additionally, the formation of high molecular weight polymers increases the viscosity of the solution, thereby reducing the rate of termination.³⁸ As seen in Figure 4B, there is a notable difference in average molecular weight, between VA:EtPAX ratios of 200:1 and 6000:1. However, increasing from a ratio of VA:EtPAX = 6000:1 to 12000:1, suggests minimal difference in the final molecular weight distribution. The limited increase in M_n while targeting higher molecular weight suggests the chain growth leveled off and molecular weights are limited by chain transfer events when it goes to higher targeted values.³⁹ The highest M_n value was achieved for VA:EtPAX = 12000:1 system and M_n value \sim 115,000 and $M_w/M_n = 1.92$. The VA:EtPAX = 6000:1 yielded polymers with M_n of 104,000 with $M_w/M_n = 1.82$, which is still substantially broader than targeted for well-controlled high molecular weight polymers. In addition to these high molecular weights, PVA polymers with $M_n > 50,000$ -80,000 and with $M_w/M_n = 1.36$ -1.44 were obtained as systems with relatively high M_n and better dispersity as seen in Table S7.



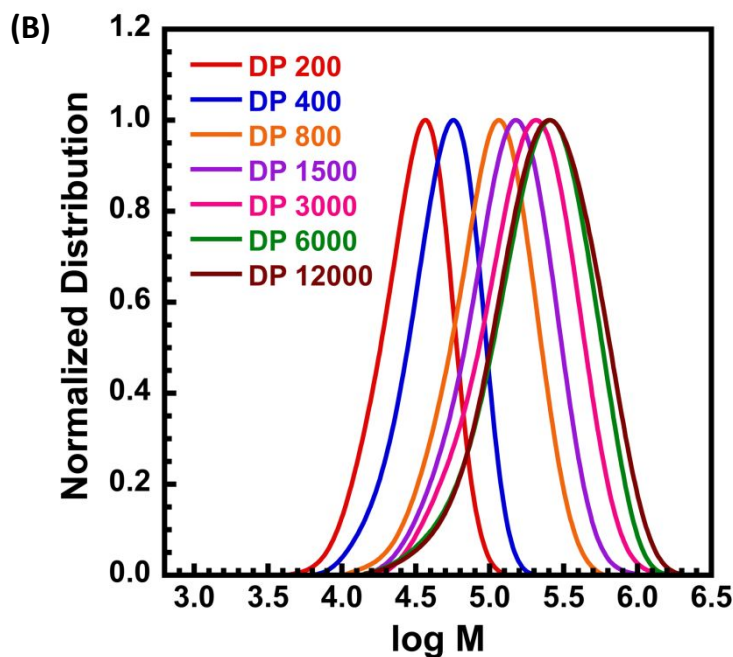


Figure 5: (A) Semilogarithmic kinetic plots for PVPiv. (B) Molecular weight distributions of PVPiv. Polymerization reactions were performed at room temperature and under blue light irradiation, using a molar ratio of $[\text{Ir}(\text{ppy})_3]/[\text{VPiv}] = 10$ ppm and $[\text{VPiv}]:[\text{EtPAX}] = \text{X}:1$ (X = The value of DP, e.g., for DP 200, X = 200).

Finally, VPiv monomer was studied with the ratio of monomer to CTA in the range of 200:1-12000:1. Figure 5A shows that the polymerization rate decreased with increasing VPiv:EtPAX ratio, similar to the observations in the PVA system. A substantial change in polymerization rate was observed at VPiv:EtPAX ratio of 12000:1. This again suggests that in high molecular weights, $\text{Ir}(\text{ppy})_3$ catalyzed PET-RAFT polymerization of vinyl esters, reduced activation from lower CTA concentrations dominates the radical generation.

When compared to PVA system, higher M_n values with better control were achieved in PVPiv system as shown in Table 1. The highest $M_n = 174,000$ with a M_w/M_n of 1.80 was achieved with a ratio of VPiv:EtPAX = 12000:1. However, even with a ratio of VPiv:EtPAX = 1500:1 gave polymers with $M_n = 107,000$ and $M_w/M_n = 1.54$. Therefore, interestingly high molecular weight polyvinyl esters of M_n greater than 170,000 were synthesized under mild

conditions using PET-RAFT polymerization of VPiv, and polymers of M_n greater than 100,000 were synthesized with $M_w/M_n \sim 1.3-1.4$ as shown in Table S7.

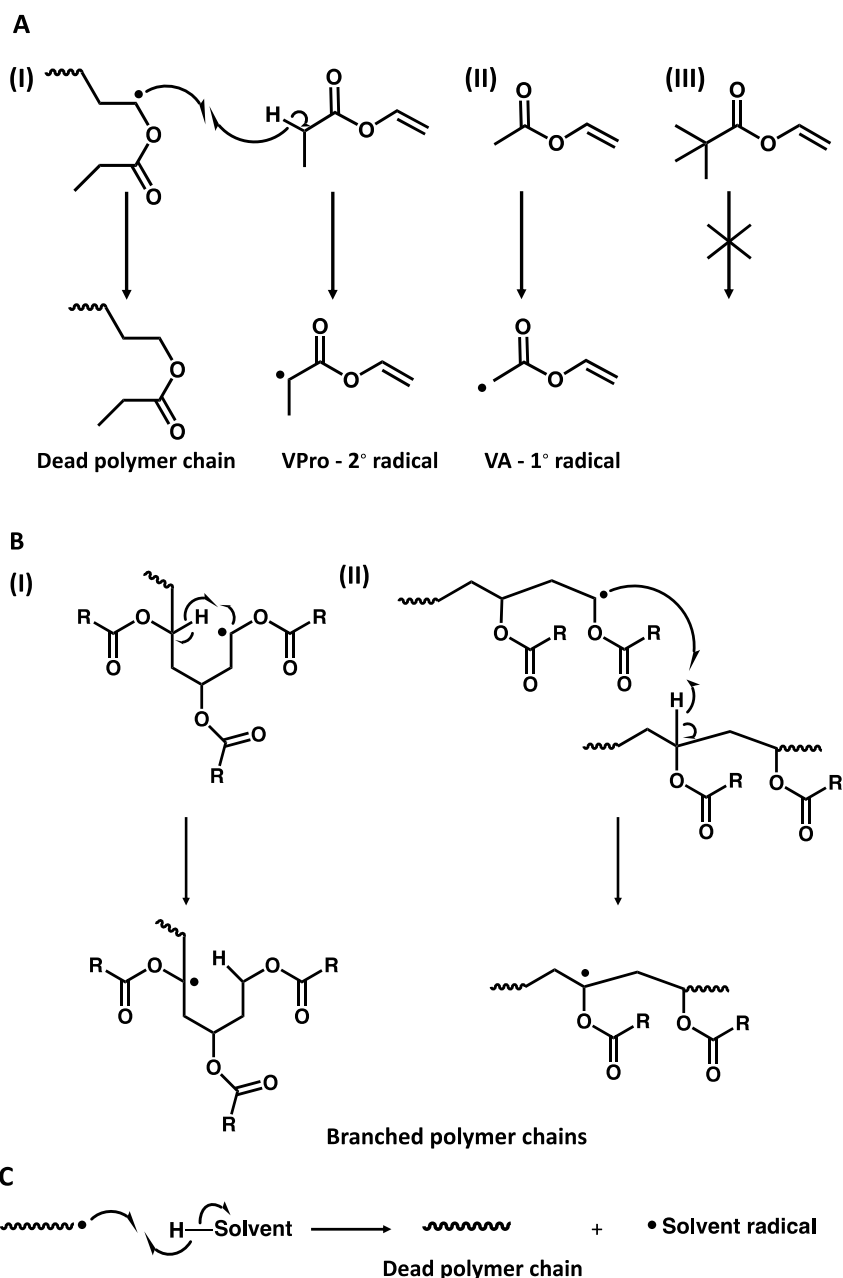
The effect of each monomer on the control of polyvinyl esters synthesized by PET-RAFT polymerization can be analyzed by comparing all three systems together. Almost same trend of polymerization rate was observed for both VA and VPiv systems. Polymerization rate mainly governed by the intrinsic propagation kinetics, radical generation, and termination rates, although side reactions such as transfer can dominate with higher ratios of monomer to CTA. Interestingly, the $\text{Ir}(\text{ppy})_3$ catalyzed PET-RAFT of VA and VPiv, appear to show a slight decrease in polymerization rate at lower CTA loadings, in contrast to the acrylate-trithiocarbonate system recently developed, where retardation effects dominated activation effects.³⁷ This could be due to the substantially higher targeted chain lengths in this study and less active xanthate RAFT agents, both causing retardation effects to be suppressed.⁴⁰ The reduction in rate at higher CTA loading is consistently seen in both PVA and PVPiv polymerization. The polymerization of VPro is poorly controlled, indicative of substantial transfer events, making such analysis challenging in that monomer.

For lower ratios of monomer to CTA, the fraction of chains impacted by side reactions is relatively small, hence chains are well-controlled by the RAFT mechanisms. Vinyl ester propagating radicals undergo α -hydrogen abstraction due to their low stability which results from the unconjugated nature of the monomer, and the limited stabilization of propagating radicals.¹⁰ Chain transfer to monomer can occur at when there is an abstractable hydrogen α to the carbonyl. Chain transfer terminates propagating chain and creates a reactive vinyl ester monomer with a radical center which can lead branching.¹¹ VPro propagating radicals have a higher susceptibility to undergo hydrogen atom abstraction from the monomer during the propagation process. As suggested in Scheme 2A, VPro propagating radical chains make more

stable 2° radical after the abstraction when compared with the VA propagating radicals which make less stable 1° radical after the abstraction. Therefore, transfer to form the 2° radical in VPro polymerization is likely to occur at a higher rate than the transfer to form a 1° radical in VA polymerization. The propensity to transfer in the VPro polymerization limits the M_n evolution and control over MWDs. Comparably, this also explains the behavior of VPiv system, because VPiv lacks abstractable hydrogens α to the carbonyl.^{41–43}

The MWDs of each polymerization system was analyzed in Table 1, comparing the theoretical and experimental M_n values for final time points. Further, M_n evolution and M_w/M_n values for each time points were shown in supporting information as Table S4, S5 and S6 for VPro, VA and VPiv, respectively. Based on the Table 1 data, the theoretical M_n and the experimental M_n values agree well for monomer:CTA values in the range of 200:1 to 800:1. However, the theoretical M_n and the experimental M_n values deviate substantially when ratio of monomer:EtPAX of 1500:1 or higher are used and this deviation is clearly observable in Figure S5. Specifically, under these conditions the experimental M_n values are substantially below the theoretical M_n values, with the suppression of M_n being most significant for VPro, followed by VA, and VPiv having the smallest deviation between experimental and theoretical M_n . This indicates how undesired side reactions, such as chain transfer reactions, limits the control over molecular weight in vinyl ester polymerization. Radical transfer to monomer through hydrogen atom abstraction is shown in Scheme 2A. This hydrogen atom abstraction is possible for VPro and VA, but not for VPiv, supporting the higher control in VPiv compared to the other monomers. Additional broadening of the MWD can occur when the highly reactive propagating radicals undergo intramolecular and intermolecular chain transfer reactions which lead for formation of long and short chain branches as shown in Scheme 2B. Although, all these polymerization reactions were carried out as near bulk polymerization reactions, formation of some dead polymers and initiation of new chains can be expected as shown in

Scheme 2C, through the chain transfer to the small amount of DMF solvent (5-7% of total volume) that is used for the preparation of Ir(ppy)₃ solution. This is consistent with the observation that polymerization of VPiv at 30 ppm led to lower M_n than polymerization at 10 ppm (Table S2).



Scheme 2: (A) Radical chain transfer between the propagating radical and the monomer (α - H abstraction). (I) Termination of VPro propagating chain to a dead chain and 2° radical after α -H abstraction. (II) 1° radical after α -H abstraction in the termination of VA propagating

radical. (III) VPiv monomer with no α -H. (B) Chain transfer to polymer. (I) Intramolecular chain transfer reaction. (II) Intermolecular chain transfer reaction. (C) Chain transfer to solvent.

Table 1: Results for PVPro, PVA, and PVPiv synthesized by PET-RAFT polymerization.

Monomer	DP	Time/h	Conversion	M_n gpc	M_w/M_n	M_n theory
			%	(g/mol)		(g/mol)
VPro	200	24	82	21800	1.86	16400
	400	24	68	26300	1.83	27300
	800	24	66	50300	1.93	52800
	1500	24	79	60800	2.18	118100
	3000	24	73	66700	2.29	219000
	6000	24	67	88700	2.00	402800
VA	200	24	89	18600	1.34	15300
	400	24	85	36700	1.29	29400
	800	24	87	46400	1.46	59700
	1500	24	84	58600	1.58	108100
	3000	24	75	81100	1.84	193500
	6000	24	75	104000	1.82	389900
	12000	24	74	115000	1.92	769200
VPiv	200	15	83	26800	1.30	21200
	400	15	80	40400	1.33	40800
	800	15	80	83500	1.48	81500
	1500	15	78	107000	1.54	150700
	3000	15	76	137000	1.65	290800
	6000	15	72	164000	1.73	556100
	12000	15	63	174000	1.80	974800

To further explore the impact of solvent on the control polymerization and growth of M_n , VPiv polymerizations targeting ratios of VPiv:EtPAX from 1500:1 to 12000:1 were performed in the presence of same amount of $\text{Ir}(\text{ppy})_3$ (10 ppm relative to monomer) photocatalyst but using 5000 ppm $\text{Ir}(\text{ppy})_3$ stock solution. This leads to $\sim 1\%$ DMF in the reaction mixture, compared to initially used 1000 ppm $\text{Ir}(\text{ppy})_3$ stock solution, which leads to $\sim 5\%$ DMF in the reaction mixture. Pleasingly, substantially higher molecular weight polymers were created with 1% DMF in solution than the polymers synthesized with 5% DMF. The M_n control was superior at 1% DMF, with comparable or even lower M_w/M_n values. As seen in Figure 6, the MWDs of polymers shifted to higher molecular weight side, with 1% DMF yielding polymers with $M_n = 145,000$ ($M_w/M_n = 1.50$), $M_n = 193,000$ ($M_w/M_n = 1.65$), $M_n = 293,000$ ($M_w/M_n = 1.65$) and $M_n = 354,000$ ($M_w/M_n = 1.89$) for the ratios of VPiv:EtPAX from 1500:1 to 12000:1 respectively. This can be compared to the 5% system which gives polymers with $M_n = 107,000$ ($M_w/M_n = 1.54$), $M_n = 137,000$ ($M_w/M_n = 1.65$), $M_n = 164,000$ ($M_w/M_n = 1.73$) and $M_n = 174,000$ ($M_w/M_n = 1.80$) for the ratios of VPiv:EtPAX from 1500:1 to 12000:1 respectively. In addition to that all these high molecular weight polymers resulted with 1% DMF have $M_w/M_n > 1.9$ and conversion higher than 70% which is useful in industrial applications. Furthermore, these data indicate the critical role played by chain transfer to solvent events even with the trace amounts of DMF. Stockmayer and coworkers have studied chain transfer constants in vinyl acetate polymerization to different substance and they have determined the transfer constant to vinyl acetate monomer is 0.00025 and transfer constant to DMF is 0.005,⁴⁴ while a plot of $1/M_n$ vs $1/M_{n\text{-Theory}}$ (Figure S6) estimates a similar transfer constant of 0.015, which is in the same order of magnitude for this system. This higher transfer constant of VA to DMF solvent implies that chain transfer to solvent is more prominent than chain transfer to monomer in vinyl acetate polymerization. Although these polymerization reactions performed in near bulk condition, the presence of trace amount of DMF in the system

led to a measurable amount of chain transfer events. The chain transfer to DMF as a solvent estimate in Table S9 are 0.022 for VPro, 0.015 for VA and 0.01 for VPiv, following the anticipated trend.

Especially, this effect can be clearly observed when considering the M_n of DP 12000 system with 1% DMF is almost two times higher than the same system with 5% DMF. In addition to chain transfer constant of DMF, Stockmayer and coworkers have reported 0.0006, 0.0025, 0.00013 and 0.001 chain transfer constant values for methanol, ethanol, tert-butanol, and acetonitrile like common solvents respectively.⁴⁴ In spite of the fact that their chain transfer constant values are lower than the chain transfer constant of DMF, Boyer and coworkers have found that methanol is less efficient as a solvent for vinyl ester polymerization and only 20% conversion was obtained after 22 h and in the presence of high catalyst loading (50 ppm with respect to monomer). Furthermore, 45% and 74% conversions were obtained in their study in acetonitrile solvent and in the presence of 20 ppm and 50 ppm catalyst loadings respectively.²⁸ However, they have obtained good control in the presence of DMSO as the solvent. The DP 1500-VPiv system was compared in the presence of 5% DMF and 5% DMSO. As seen in Table S8, $M_n = 172,800$ with $M_w/M_n = 1.73$ and $M_n = 107,300$ with $M_w/M_n = 1.54$ were resulted for 5% DMSO and 5% DMF respectively with minimal difference when compared both M_n and dispersity.

All these transfer processes can broaden molecular weight distributions and can cause lower experimental M_n values compared to their theoretical values. The impact of these side reactions is especially significant at lower ratios of CTA to monomer, since the fraction of controlled chains will be lower, due to the lower concentration of CTA. Importantly, we are the first who reported the vinyl ester polymers with molecular weights higher than 350,000 and $M_w/M_n < 1.9$ by any RAFT technique to the best of our knowledge.

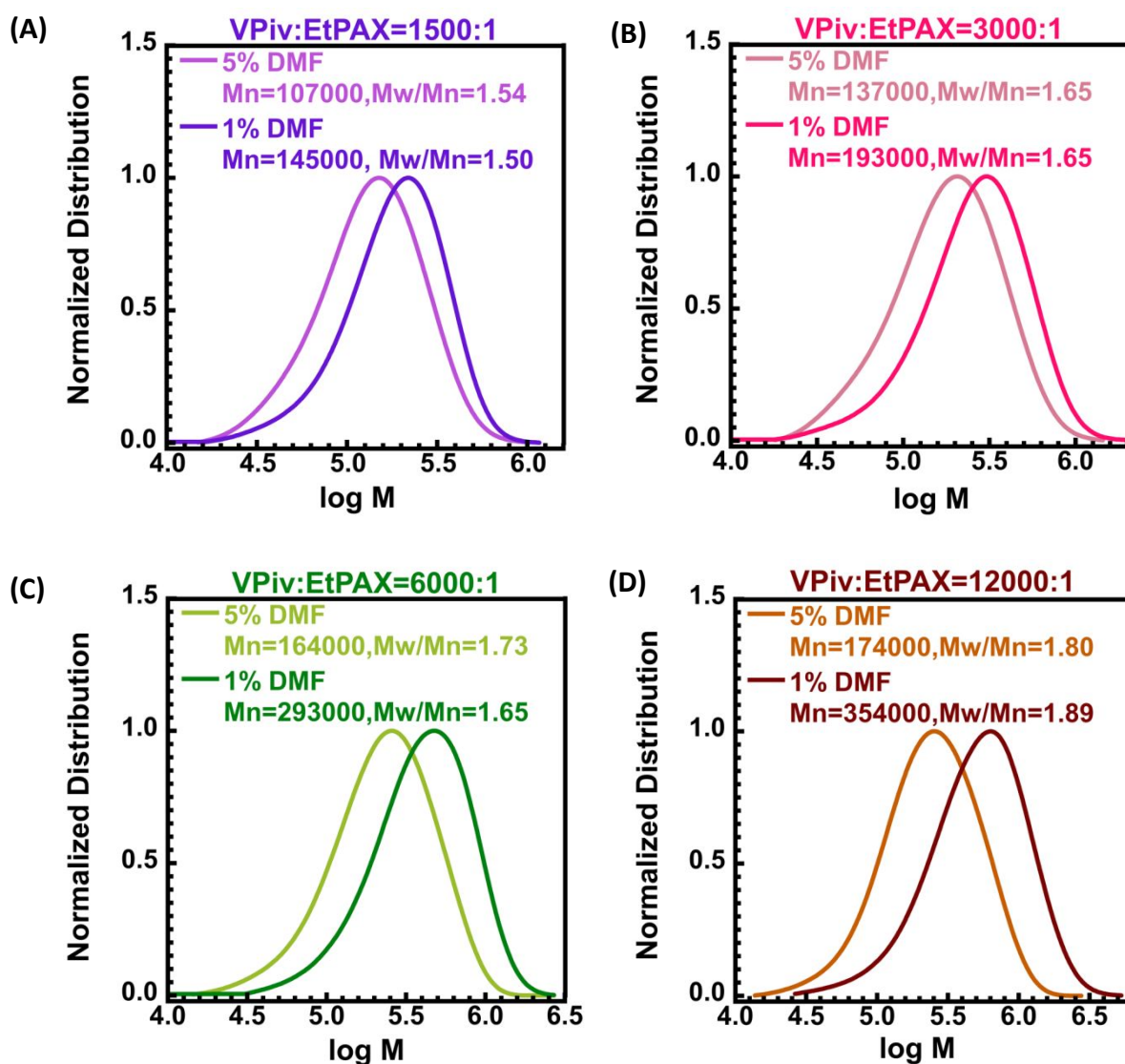


Figure 6: Molecular weight distributions for VPiv polymerization in the presence of 5% and 1% DMF as the solvent for the Ir(ppy)₃ solution. (A) Target DP 1500. (B) Target DP 3000. (C) Target DP 6000. (D) Target DP 12000. Polymerization reactions were performed at room temperature and under blue light irradiation, using a molar ratio of [Ir(ppy)₃]/[VPiv] = 10 ppm and [VPiv]:[EtPAX] = X:1 (X = The value of the Target DP, e.g., for Target DP 1500, X = 1500).

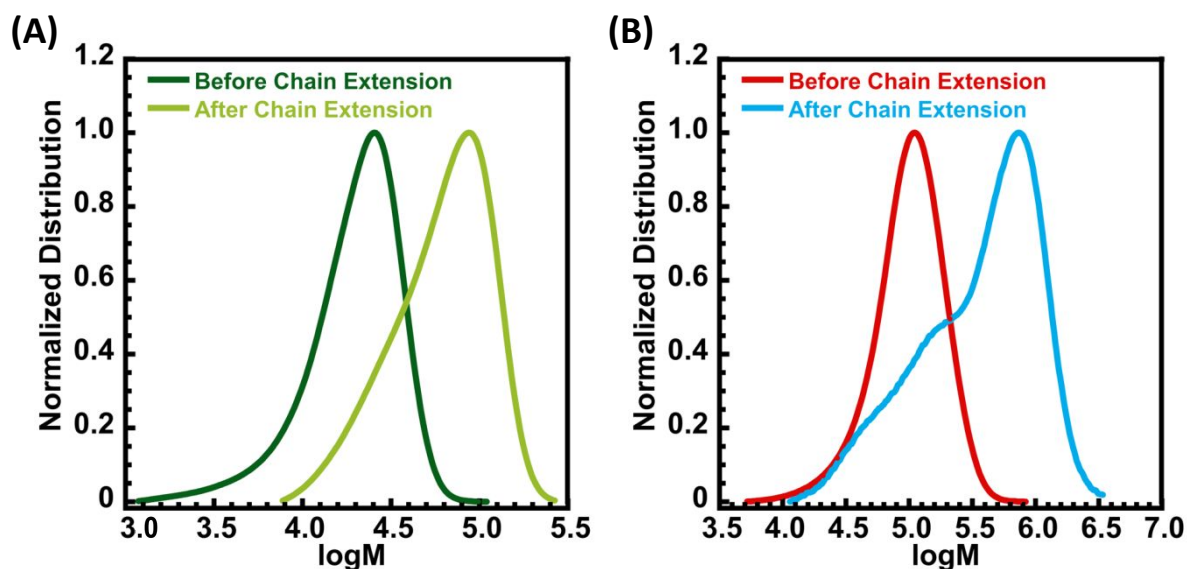


Figure 7: (A) Molecular weight distributions before -DP 200 (synthesis of macro-CTA) and after chain extension-DP 400. (B) Molecular weight distributions before -DP 1500 (synthesis of macro-CTA) and after chain extension-DP 6000. All polymerization reactions were performed at room temperature and under blue light irradiation.

Beyond control over primary chain length, the livingness of a polymer was explored. Living polymers grow in the presence of more monomer and have gained the interest in the synthesis of block polymers because they can offer precision in macromolecular structure by controlling the molecular weight and MWDs.^{45,46} The livingness of low and high targeted chain lengths of vinyl ester polymers synthesized from PET-RAFT polymerization were studied using two chain extension reactions. In the first chain extension reaction, the macro-CTA was synthesized using CTA:VPiv monomer = 1:200 (DP 200) and it was extended following macro-CTA:VPiv monomer = 1:400 (DP 400). The ratio of CTA:VPiv = 1:1500 was used to synthesize the macro-CTA for the second chain extension reaction and it was extended into DP 6000 following the ratio of macro-CTA:VPiv = 1:6000. The MWDs before and after chain extension are shown in Figure 7A and 7B for the systems with DP 200 and DP 1500 macro-CTAs respectively. In the first chain extension started with low DP value, the macro-CTA had $M_n = 15,500$ and $M_w/M_n = 1.46$ with 62% monomer conversion, and after the chain extension the final polymer with $M_n = 49,200$ and $M_w/M_n = 1.47$ with 51% monomer conversion was

resulted. This clearly demonstrated the livingness of the macro-CTA synthesized using the DP 200 system. The polymer with $M_n = 78,300$, $M_w/M_n = 1.50$ and 64% conversion was obtained after performing the polymerization for 1:1500 = CTA:VPiv monomer ratio as the macro-CTA for the second chain extension reaction. This macro-CTA was extended using the ratio of 1:6000 = macro-CTA:VPiv monomer. As seen in Figure 7B, after the chain extension, the MWD of the polymer has shifted to higher molecular weight side with a shoulder peak at the low molecular weight end. The extended polymer had $M_n = 180,900$, $M_w/M_n = 3.00$ and 15% conversion. Furthermore, the extended peak was deconvoluted to determine the extended percent and the control of the macro-CTA synthesis at DP 1500. Two distributions with $M_n = 127,100$ and $M_w/M_n = 2.88$ with area peak % = 57% and $M_n = 728,300$, $M_w/M_n = 1.26$ and area peak % = 43% were estimated after the deconvolution. This extension clearly demonstrated that at high targeted chain length of vinyl ester polymerization ($DP \geq 1500$), only around ~50% chains are living because only a fraction of macro-CTA has extended into really high molecular weight polymer with $M_n = 728,300$ and narrow MWD ($M_w/M_n = 1.26$) as seen in Figure 7C. Especially, when considering Table 1 and Figure S5, the deviation between experimental M_n and theoretical M_n is more prominent (~30%) starting from DP 1500 because of low CTA loading and thereby undesirable chain transfer reactions being more dominant. However, for systems with low DP (DP 200-DP 800) the experimental M_n agrees with the theoretical M_n value as seen in Figure S5, because of high CTA:Monomer ratio and thereby better control in the polymerization. Therefore, chain extension reactions shown in Figure 7 indicate the better control and high-end group fidelity in low DP systems and less control and low-end group fidelity in high DP systems in vinyl ester polymerization.

Conclusion

This study reports the effect of monomer type on the evolution of M_n and MWD for PET-RAFT polymerization of vinyl ester monomers. The vinyl ester propagating radicals are prone to transfer reactions during the polymerization because of their high reactivity and limited stabilization of the propagating radical. The precision of vinyl ester polymerization was best for VPiv, followed by VA with lowest control in VPro. The control over the polymerization follows the susceptibility towards chain transfer reactions. Especially, chain transfer to solvent is more noticeable and M_n increases more in the presence of less amount of solvent. PET-RAFT polymerization can control the polymerization of vinyl esters when compared with other polymerization techniques synthesizing high molecular weight polyvinyl esters (e.g., PVPiv with $M_n > 350,000$ and PVA with $M_n > 80,000$) under mild conditions. The deviation between experimental and theoretical M_n is significant at DP 1500 system of vinyl ester polymerization and furthermore this is confirmed by only ~ 50% chains are extended into high molecular weight polymers during the chain extension. Furthermore, the livingness and better control in low DP system was confirmed by chain extension reaction successfully.

Acknowledgements

We are grateful to Dr. Kate Bradford for experimental assistance with the synthesis of EtPAX. This work was partially supported by the National Science Foundation under award number CHE-2203727. 400 MHz NMR Instrumentation at Miami University is supported by the National Science Foundation under award number CHE-1919850.

References

- 1 R. W. Nunes, J. R. Martin and J. F. Johnson, *Polym Eng Sci*, 1982, **22**, 205–228.

- 2 T. Kida, R. Tanaka, Y. Hiejima, K. Nitta and T. Shiono, *Polymer (Guildf)*, 2021, **218**, 123526.
- 3 T. Shimizu, N. P. Truong, R. Whitfield and A. Anastasaki, *ACS polymers Au*, 2021, **1**, 187–195.
- 4 A. Kaboorani and B. Riedl, in *Biocomposites*, Elsevier, 2015, pp. 347–364.
- 5 W. Lyoo and H. Lee, *Colloid Polym Sci*, 2002, **280**, 835–840.
- 6 S. Perrier and P. Takolpuckdee, *J Polym Sci A Polym Chem*, 2005, **43**, 5347–5393.
- 7 D. Boschmann and P. Vana, *Polymer Bulletin*, 2005, **53**, 231–242.
- 8 J. Hwang, H.-C. Lee, M. Antonietti and B. V. K. J. Schmidt, *Polym Chem*, 2017, **8**, 6204–6208.
- 9 M. Kamigaito, *Polym J*, 2022, 1–15.
- 10 S. Perrier, *Macromolecules*, 2017, **50**, 7433–7447.
- 11 S. Harrisson, X. Liu, J.-N. Ollagnier, O. Coutelier, J.-D. Marty and M. Destarac, *Polymers (Basel)*, 2014, **6**, 1437–1488.
- 12 M. Abdollahi, P. Bigdeli, M. Hemmati, M. Ghahramani and M. Barari, *Polym Int*, 2015, **64**, 1808–1819.
- 13 K. Koumura, K. Satoh, M. Kamigaito and Y. Okamoto, *Macromolecules*, 2006, **39**, 4054–4061.
- 14 G. Mazzotti, T. Benelli, M. Lanzi, L. Mazzocchetti and L. Giorgini, *Eur Polym J*, 2016, **77**, 75–87.
- 15 H. Tang, M. Radosz and Y. Shen, *AIChE journal*, 2009, **55**, 737–746.
- 16 C.-H. Peng, J. Scricco, S. Li, M. Fryd and B. B. Wayland, *Macromolecules*, 2008, **41**, 2368–2373.
- 17 S. Shanmugam and K. Matyjaszewski, in *Reversible Deactivation Radical Polymerization: Mechanisms and Synthetic Methodologies*, ACS Publications, 2018, pp. 1–39.
- 18 N. Corrigan, K. Jung, G. Moad, C. J. Hawker, K. Matyjaszewski and C. Boyer, *Prog Polym Sci*, 2020, **111**, 101311.
- 19 S. Harrisson, X. Liu, J.-N. Ollagnier, O. Coutelier, J.-D. Marty and M. Destarac, *Polymers (Basel)*, 2014, **6**, 1437–1488.
- 20 D. Mardare and K. Matyjaszewski, *Macromolecules*, 1994, **27**, 645–649.

- 21 G. Moad, E. Rizzardo and S. H. Thang, *Aust J Chem*, 2005, **58**, 379–410.
- 22 J. Chiefari, Y. K. Chong, F. Ercole, J. Krstina, J. Jeffery, T. P. T. Le, R. T. A. Mayadunne, G. F. Meijs, C. L. Moad and G. Moad, *Macromolecules*, 1998, **31**, 5559–5562.
- 23 J. P. Russum, N. D. Barbre, C. W. Jones and F. J. Schork, *J Polym Sci A Polym Chem*, 2005, **43**, 2188–2193.
- 24 R. W. Simms, T. P. Davis and M. F. Cunningham, *Macromol Rapid Commun*, 2005, **26**, 592–596.
- 25 F. Zhao, A. R. Mahdavian, M. B. Teimouri, E. S. Daniels, A. Klein and M. S. El-Aasser, *Colloid Polym Sci*, 2012, **290**, 1247–1255.
- 26 R. Li and Z. An, *Angewandte Chemie International Edition*, 2020, **59**, 22258–22264.
- 27 R. N. Carmean, T. E. Becker, M. B. Sims and B. S. Sumerlin, *Chem*, 2017, **2**, 93–101.
- 28 S. Shanmugam, J. Xu and C. Boyer, *Macromolecules*, 2014, **47**, 4930–4942.
- 29 D. Britton, F. Heatley and P. A. Lovell, *Macromolecules*, 1998, **31**, 2828–2837.
- 30 T. G. McKenzie, Q. Fu, M. Uchiyama, K. Satoh, J. Xu, C. Boyer, M. Kamigaito and G. G. Qiao, *Advanced Science*, 2016, **3**, 1500394.
- 31 M. L. Allegrezza and D. Konkolewicz, *ACS Macro Lett*, 2021, **10**, 433–446.
- 32 X. Pan, M. A. Tasdelen, J. Laun, T. Junkers, Y. Yagci and K. Matyjaszewski, *Prog Polym Sci*, 2016, **62**, 73–125.
- 33 N. D. Dolinski, Z. A. Page, E. H. Discekici, D. Meis, I. Lee, G. R. Jones, R. Whitfield, X. Pan, B. G. McCarthy and S. Shanmugam, *J Polym Sci A Polym Chem*, 2019, **57**, 268–273.
- 34 S. Perrier and P. Takolpuckdee, *J Polym Sci A Polym Chem*, 2005, **43**, 5347–5393.
- 35 K. Hakobyan, T. Gegenhuber, C. S. P. McErlean and M. Müllner, *Angewandte Chemie International Edition*, 2019, **58**, 1828–1832.
- 36 S. Perrier, *Macromolecules*, 2017, **50**, 7433–7447.
- 37 B. Parnitzke, T. Nwoko, K. G. E. Bradford, N. D. A. Watuthanthrige, K. Yehl, C. Boyer and D. Konkolewicz, *Chemical Engineering Journal*, 2023, **456**, 141007.
- 38 G. Johnston-Hall and M. J. Monteiro, *J Polym Sci A Polym Chem*, 2008, **46**, 3155–3173.
- 39 J. T. Clarke, R. O. Howard and W. H. Stockmayer, *Die Makromolekulare Chemie: Macromolecular Chemistry and Physics*, 1961, **44**, 427–447.

- 40 K. G. E. Bradford, L. M. Petit, R. Whitfield, A. Anastasaki, C. Barner-Kowollik and D. Konkolewicz, *J Am Chem Soc*, 2021, **143**, 17769–17777.
- 41 N. Kubota, A. Kajiwara, P. B. Zetterlund, M. Kamachi, J. Treurnicht, M. P. Tonge, R. G. Gilbert and B. Yamada, *Macromol Chem Phys*, 2007, **208**, 2403–2411.
- 42 E. Girard, X. Liu, J.-D. Marty and M. Destarac, *Polym Chem*, 2014, **5**, 1013–1022.
- 43 T. Yamamoto, S. Yoda, O. Sangen, R. Fukae and M. Kamachi, *Polym J*, 1989, **21**, 1053–1054.
- 44 J. T. Clarke, R. O. Howard and W. H. Stockmayer, *Die Makromolekulare Chemie: Macromolecular Chemistry and Physics*, 1961, **44**, 427–447.
- 45 R. B. Grubbs and R. H. Grubbs, *Macromolecules*, 2017, **50**, 6979–6997.
- 46 H. S. Wang, N. P. Truong, Z. Pei, M. L. Coote and A. Anastasaki, *J Am Chem Soc*, 2022, **144**, 4678–4684.